PAPER

Check for updates

A thiol-containing zirconium MOF functionalized with silver nanoparticles for synergistic CO_2 cyclo-addition reactions†

Rajesh Patra and Debajit Sarma [ID] *

Thiol-containing biomolecules, such as cysteine and glutathione, play essential roles in regulating the polarity and reactivity of the systems. Among functional MOFs, thiol MOFs, a subclass with a thiol group-containing ligand, are relatively less explored due to their synthetic challenges and stability and storage issues. Despite these drawbacks, they have many advantages due to the electronically soft thiol groups with strong reactivity and affinity toward soft metal ions. Herein, we have taken advantage of the affinity between thiol groups and a soft metal (Ag) by functionalizing a thiol MOF with Ag ions and finally synthesizing a silver nanoparticle-functionalized heterogeneous catalyst (Ag@Zr-DMBD). The Zr,Ag centre of the thiol MOF catalyst acts as an active centre and synergistically binds with the electron-rich oxygen atom of a terminal epoxide for efficient CO_2 fixation to the corresponding cyclic carbonates under atmospheric CO_2 pressure in 8 h. Finally, a rationalized reaction mechanism is proposed based on literature reports and current results. This work presents a viable strategy for using thiol MOFs as heterogeneous catalysts for CO_2 fixation under mild conditions.

Introduction

Metal–organic frameworks (MOFs) are a class of porous materials formed by the combination of metal ions or nodes and organic linkers.[1–5] MOFs have received substantial interest in the field of porous materials during the last three decades due to their unique properties such as high crystallinity,[6] porosity,[7] large surface area,[8] *etc.* and applicability in a variety of disciplines, such as gas storage and separations,[9–11] conductivity,[12] drug delivery,[13] catalysis,[14–18] sensing,[19–23] and many others.[24–27] The presence of the inorganic nodes and organic linkers in the MOF structure has given the advantage of tuning both the inorganic and organic parts for a desired application. Ligands containing carboxylic groups and N-based donor centres constitute the two major classes of ligands for MOF structures. Similarly, over the years, carboxylic acid ligands containing different functional groups such as alkyl(–R),[28] halogen (–X),[29] amine (–NH$_2$),[30] and alcohol (–OH)[31] groups have been utilized predominantly. In this category of functional MOFs, thiol group (–SH) containing MOFs are relatively less explored due to the scarcity of thiol-based ligands, synthetic challenges, and storage issues.[32,33] The thiol or sulfhy-

dryl group is an important functional group in chemistry and biology.[34] Cysteine, a thiol-containing amino acid, plays an essential role in the formation and reactivity of almost all enzymes and proteins.[35] Similarly, thiol-rich proteins store and transport many essential cations (Cu^{2+}, Zn^{2+}, *etc.*) in humans.[36] Free thiol-containing glutathione (GSH) acts as an antioxidant in plants.[37] Several enzymes use thiol groups as active sites, which allows them to bind with metal cations and increase their catalytic activity.[38] Hence, thiol-based MOFs are an area of immense interest but still relatively unexplored.[39]

Bi-functional ligands (containing carboxylic-acid and thiol acid groups) such as 2,5-dimercaptoterephthalic acid (H$_2$DMBD),[32] 3,3′-dimercapto-1,1′-biphenyl-4,4′-dicarboxylic acid (H$_2$DMBPD),[40] 4,4′,4″,4‴-(pyrene-1,3,6,8-tetrayl)tetrakis(2,6-dimercaptobenzoic acid) (H$_4$OMTP)[41] *etc.*, are commonly used as thiol-based ligands for synthesizing thiol MOFs. As the thiol ligands contain two electronically different functional groups (–COOH as an electronically hard functional group and –SH as an electronically soft functional group), the electronic nature of metal ions plays a distinct role in the synthesis and structure of thiol MOFs, as hard metal ions bind with an electronically hard functional group and soft metal ions bind with soft functional groups in accordance with the HSAB principle. For synthesizing MOFs with free thiol groups, an electronically hard metal such as zirconium (Zr) is used exclusively.[32,40,41] In 2013, Xu and co-workers reported the first stable thiol MOF, Zr-DMBD, by the reaction between ZrCl$_4$ and 2,5-dimercapto-

Department of Chemistry, Indian Institute of Technology Patna, Bihar 801106, India. E-mail: debajit@iitp.ac.in, rajesh_1921ch07@iitp.ac.in

†Electronic supplementary information (ESI) available. See DOI: https://doi.org/10.1039/d3dt01583a

terephthalic acid (H₂DMBD), which forms an isoreticular framework of UiO-66.[32,42] As the Zr metal ion is electronically hard, it only bonds with electronically hard carboxylic acid groups, and the thiol groups remain free-standing in the MOF structure. By utilizing the free-standing thiol groups of the stable MOF, Zr-DMBD was used for various applications such as heavy metal adsorption,[32] photocatalysis,[43] heterogeneous catalysis,[44] *etc*. Many studies have used Zr-DMBD as a Hg adsorbent due to the propensity of the free thiol group to form a covalent bond with electronically soft mercury ions.[32,45] Xu and co workers have demonstrated the application of Zr-DMBD for efficient Hg adsorption.[32] In 2018, Sun and co-workers studied the Hg adsorption mechanism of Zr-DMBD.[46] Phang *et al.* studied the super protonic conductivity of Zr-DMBD analogues.[47] In 2018, Liu *et al.* reported the photocatalytic conversion of CO_2 to CO, using Co-anchored Zr-DMBD.[43] The application of thiol MOFs for heterogeneous catalysis is relatively unexplored.[48] However, because they contain an electronically soft thiol functional group that can anchor many catalytically active metal centres such as Pd, Ag, and Au, there is a real possibility that they could be used as catalysts for effective organic transformations.[49–53]

Atmospheric CO_2 concentrations are rising steadily and have already surpassed 400 ppm, causing severe environmental concerns, *viz.*, global warming, climate change, ocean acidification, *etc*.[54,55] Even though several CO_2-absorbent materials have been developed over the years, it's clear that this is not a fool-proof strategy for dealing with the problem.[56–58] Much work is being done to find ways to put carbon dioxide to use that will help mitigate the issue, such as making valuable chemicals and fuels out of it.[59–61] However, the high thermodynamic stability and kinetically inert nature of CO_2 make the process challenging.[62,63] Hence, developing efficient heterogeneous catalysts for carbon capture and its utilization (CCU) has attracted significant attention in the past few decades.[64,65] Mainly, synthesis of cyclic carbonates from epoxides has attracted considerable attention because of their applications as fine chemicals in pharmaceutical industries, starting materials in polymer industries, electrolytes in battery industries, *etc*.[66,67] Over the years, zeolites,[68] porous-organic polymers (POPs),[69] coordination organic frameworks (COFs),[70,71] metal–organic frameworks (MOFs),[72–77] and nanoparticle supported materials[49–53,78] have been utilized for the conversion of epoxides to cyclic carbonates. Still, due to the chemical inertness of CO_2, the utilized reaction conditions in these catalysts are relatively harsh.[79]

Silver-based materials are well known for CO_2 fixation reactions.[80–86] In particular, for catalytic conversion of terminal epoxides to cyclic carbonates, different silver complexes,[87] silver-based MOFs,[85] and silver nanoparticle incorporated materials have been utilized.[83,84,86,88] In a recent report Li *et al.* demonstrated that silver active sites surrounded by gold nanoclusters show efficiency in the ring-opening of epoxides, and the incorporation of CO_2 can act as a driving force for the conversion.[89] Still detailing the use of silver-containing materials in the cycloaddition of epoxides is primarily an uncharted territory. So, synthesizing a new silver nanoparticle containing heterogeneous catalyst for converting terminal epoxides to cyclic carbonates is advantageous.

Herein, we have successfully synthesized a well-known stable thiol MOF Zr-DMBD and utilized its free-standing thiol group to functionalize with the catalytically active metal centre Ag(I) followed by reduction to Ag nanoparticles. The Ag nanoparticle functionalized thiol MOF Ag@Zr-DMBD was utilized for the CO_2 fixation reaction. The catalyst reaches its maximum conversion capacity (>99%) in 8 hours at ambient pressure and temperature for the model reaction. Due to the presence of the electronically soft thiol group (–SH) in the MOF structure, it can easily form a covalent bond with the electronically soft Ag centre, which prevents the catalyst from leaching during the reaction.

Experimental sections

Materials and methods

All commercially available reagents were purchased from different sources and used without further purification. 2,5-Dihydroxyterephthalic acid diethyl ester and anhydrous dimethylformamide (DMF) were acquired from Sigma Aldrich Corporation. CDH Chemicals supplied 1,4-diazabicyclo[2.2.2]-octane (DABCO), tetrabutylammonium bromide (TBAB), dichloromethane (DCM) and silver nitrate ($AgNO_3$). TCI India Corporation was the source of all terminal epoxides.

### Synthesis and characterization

Synthesis of the thiol ligand 2,5-dimercaptoterephthalic acid (H₂DMBD). The thiol-based ligand 2,5-dimercaptoterephthalic acid (H₂DMBD) was synthesized by a three-step organic transformation following the previously reported procedure.[32,46,90] The details of the organic transformation are given in the ESI,† and it was characterized by ¹H NMR (Fig. S1–3†).

Synthesis of the catalyst Ag@Zr-DMBD. The silver-functionalized catalyst Ag@Zr-DMBD was synthesized by post-synthetic silver nanoparticle functionalization in the well-known stable thiol MOF Zr-DMBD which was synthesized following the reported procedure given in the ESI.†[32,46] A solution impregnation method was utilized to synthesize the catalyst (Scheme 1).[91] Briefly, 50 mg of Zr-DMBD was stirred for 8 hours in an acetonitrile solution with a certain amount of $AgNO_3$ to obtain Zr-DMBD–Ag(I). Finally, reducing Zr-DMBD–Ag(I) with $NaBH_4$ leads to the silver nanoparticle functionalized catalyst Ag@Zr-DMBD. Detailed synthetic procedures are given in the ESI.†

Results and discussion

Structure of Zr-DMBD

The stability of the metal–organic framework (MOF) UiO-66 (UiO = University of Oslo) reported in 2008 by Lillerud and co-workers was a significant milestone.[42] It was synthesized by
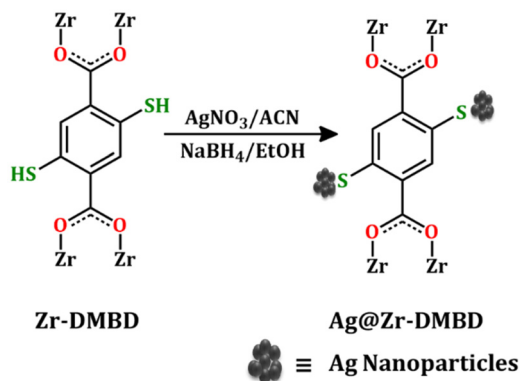
Scheme 1 Synthesis of the Ag nanoparticle functionalized thiol MOF Ag@Zr-DMBD.

reacting 1,4-benzenedicarboxylic acid (H_2BDC) with $ZrCl_4$. The formula of UiO-66 is $Zr_6O_4(OH)_4(BDC)_6$, where 1,4-benzenedicarboxylate struts are connected to $Zr_6O_4(OH)_4$ clusters as 12-connected nodes. Zr-DMBD, with the chemical formula $Zr_6O_4(OH)_4(DMBD)_6$, is isostructural to UiO-66 (Fig. 1), which is confirmed by the PXRD pattern.[32] In the Zr-DMBD structure, the carboxylic group is connected to the electronically hard Zr cluster, and the electronically soft thiol group remains a reactive free-standing group.

Characterization

The phase purity of the as-synthesized thiol MOF Zr-DMBD was analyzed by powder X-ray diffraction (PXRD). The PXRD peaks perfectly match with the simulated UiO-66 (comprises $Zr_6O_4(OH)_4$ clusters as 12 linked nodes and linear 1,4-benzene-dicarboxylate struts) patterns which confirm the phase purity of the synthesized Zr-DMBD (Fig. 2a). The FTIR spectra of Zr-DMBD show the corresponding thiol peak at 2555 cm^{-1}, confirming the presence of free-standing thiol groups (Fig. 2b). The Ag functionalization in the thiol group of Zr-DMBD was confirmed by SEM analysis (Fig. 2c and Fig. S4†), which is also
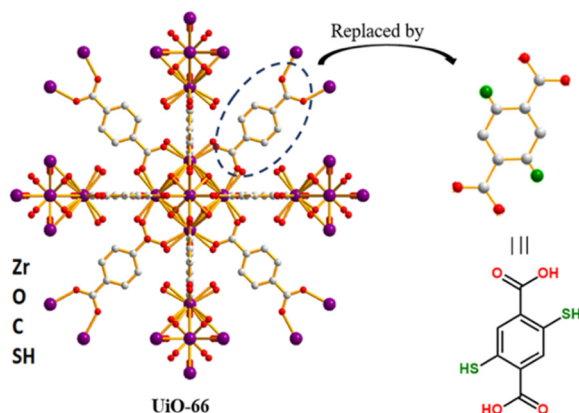

Fig. 1 Structure of UiO-66 and replacement of the organic linker by the thiol linker (DMBD) to form the thiol-MOF with a UiO-66 topology (drawn by modifying the CIF file Information card for entry 4512072).

supported by IR spectroscopy where the –S–H peak of the parent compound is diminished (Fig. 2b). The PXRD pattern of the corresponding catalyst Ag@Zr-DMBD also matches well with that of Zr-DMBD (Fig. 2a), confirming the framework's stability but the absence of any characteristics peak of Ag nanoparticle indicates the low loading of Ag nanoparticles.

Furthermore, FESEM analysis revealed that the cubic morphology of Zr-DMBD was retained even after Ag functionalization (Fig. 2c and Fig. S4†). The amount of Ag functionalization in the thiol MOF was examined by SEM-EDX, and it shows a 2.96 weight% loading of the Ag nanoparticles in the MOF moiety (Fig. S5†). The comparison between the TGA plots of the parent MOF Zr-DMBD, Zr-DMBD–Ag(I) and the catalyst Ag@Zr-DMBD shows that the stability of the catalyst is retained upon Ag functionalization (Fig. S6†). The size and distribution of silver nanoparticles were analyzed by TEM (Fig. 2d). In the HR-TEM image of the material, lattice fringes were observed, spaced at 0.23 nm, corresponding to the (111) plane of the Ag nanoparticle, further confirming the material's crystallinity (Fig. 2e). The average size of the spherical Ag nanoparticles is around 5.50 nm (Fig. 2f). The XPS survey spectrum confirms the presence of all elements Zr, C, O, S, and Ag (Fig. 2g). XPS analysis also confirms the presence of silver nanoparticles through the corresponding peaks of Ag $3d_{5/2}$ and Ag $3d_{3/2}$ at 368.2 and 374.2 eV, respectively (Fig. 2h).[91] The S 2p peaks of the synthesized catalyst were observed at 163.2 eV, which is shifted from the reported value of 163.5 for Zr-DMBD, confirming the interaction of thiol with silver nanoparticles, and the peak at 168.4 is due to oxidized sulfur, which could happen upon contact with the $AgNO_3$ salt (Fig. S7†).[43,92]

Gas adsorption analysis

For gas adsorption analysis, the compound was made solvent-free by immersing in methanol, changing to fresh methanol at 12 h time intervals, and finally drying in a vacuum oven for 12 h at 60 °C. N_2 adsorption measurements were carried out to confirm the microporous nature of the pristine MOF Zr-DMBD and the silver nanoparticle functionalized catalyst Ag@Zr-DMBD at 77 K. From the N_2 adsorption–desorption isotherm, it can be seen that both Zr-DMBD and Ag@Zr-DMBD show type IV plots. The as-synthesized thiol MOF Zr-DMBD shows (Brunauer–Emmett–Teller) a BET surface area of 190 m^2 g^{-1} which is close to the reported surface area of 262.81 m^2 g^{-1}.[46] The synthesized catalyst Ag@Zr-DMBD exhibits a BET surface area of 89 m^2 g^{-1} (Fig. 3a), and the reduction of the surface area in the catalyst indicates the functionalization of silver in the pristine MOF. The average pore width of the catalyst increases from 1.18 nm to 2.47 nm for Zr-DMBD to Ag@Zr-DMBD conversion (Fig. S8†). The CO_2 adsorption analysis shows 18 and 5.2 cm^3 g^{-1} uptake at 298 K (Fig. 3b) for Zr-DMBD and Ag@Zr-DMBD, respectively.

Utilization of the Ag@Zr-DMBD catalyst for solvent-free fixation of CO_2 to the corresponding cyclic carbonates

The catalyst Ag@Zr-DMBD contains catalytically active Ag nanoparticles, which can act as auxiliary binding sites for CO_2; it also contains Brønsted acidic sites (Zr-OH/OH_2) and moder-
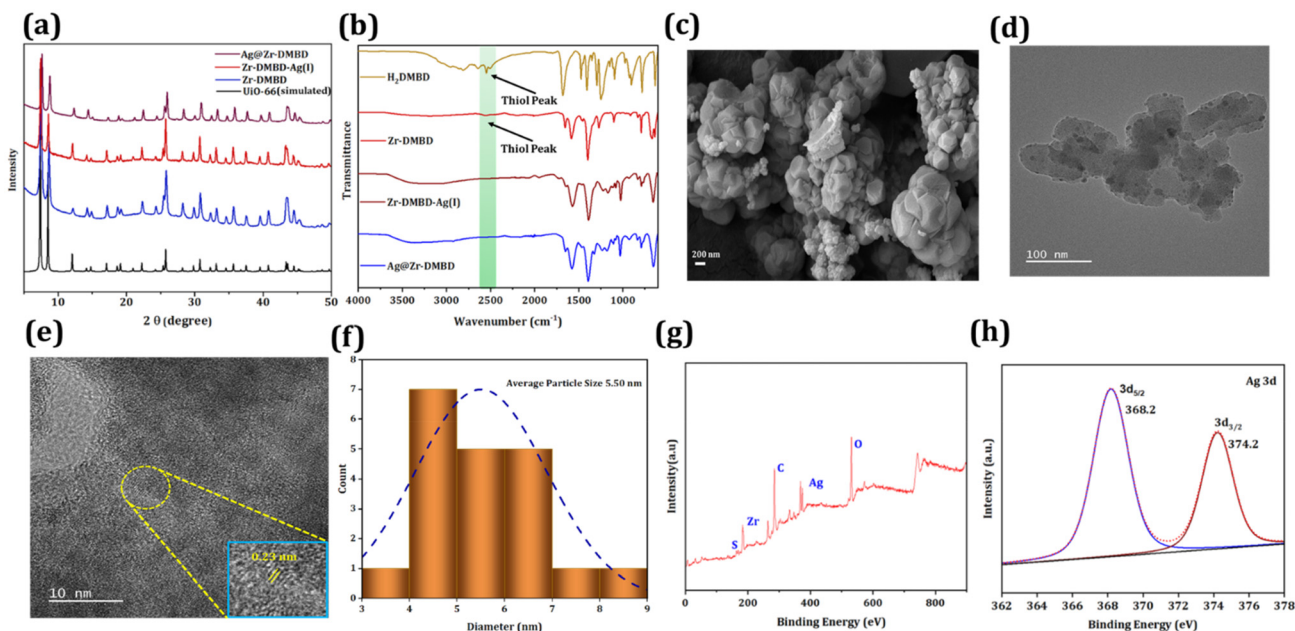
Fig. 2 (a) PXRD of simulated UiO-66, Zr-DMBD, Zr-DMBD–Ag(ɪ) and Ag@Zr-DMBD; (b) FTIR spectra of H$_2$DMBD, Zr-DMBD, Zr-DMBD–Ag(ɪ) and Ag@Zr-DMBD. (c) SEM image of the catalyst Ag@Zr-DMBD; (d) TEM image of Ag@Zr-DMBD. (e) HR-TEM images of Ag@Zr-DMBD showing fringes; (f) size distribution histogram of Ag nanoparticles; (g) survey spectrum of Ag@Zr-DMBD; (h) XPS spectra of Ag 3d.
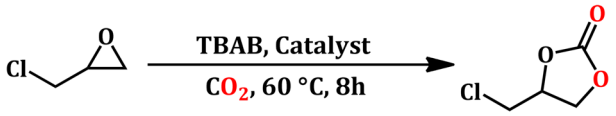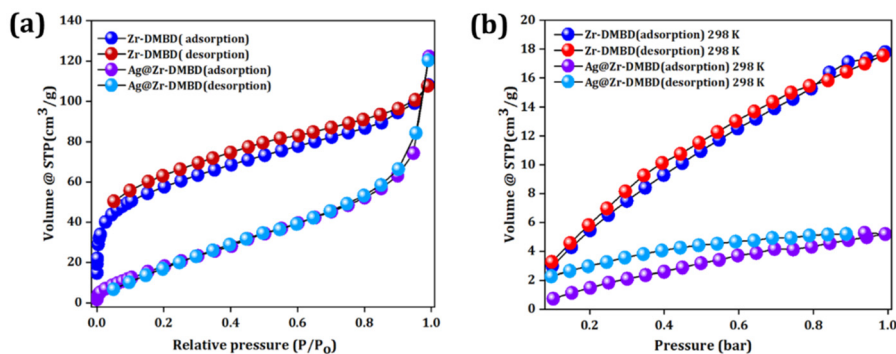

Fig. 3 (a) N$_2$ adsorption isotherms for Zr-DMBD and Ag@Zr-DMBD at 77 K and (b) CO$_2$ adsorption–desorption isotherms at 298 K.

ately polar thiol groups, which encouraged us to study the efficiency of the catalyst for CO$_2$ fixation. Therefore, the activity of the catalyst was investigated using epichlorohydrin (EPH) as a model reaction under solvent-free and atmospheric pressure conditions (1 bar CO$_2$ balloon). The initial reaction screening was done using a blank reaction (without a catalyst), which shows no conversion of the starting material to cyclic carbonate (Table 1 Sl. no. 1). The precursor materials showed no evidence of catalytic conversion (Table 1 Sl. no. 2 and 3). Silver nitrate (AgNO$_3$) alone exhibits 20% conversion of epichlorohydrin to the corresponding cyclic carbonate at 60 °C (Table 1 Sl. no. 4). On the other hand, the thiol MOF Zr-DMBD shows a low conversion of 36% without any co-catalyst (Table 1 Sl. no. 7).

So, for further enhancement of the conversion of the product, tetrabutylammonium bromide (TBAB) was chosen as

a co-catalyst. We have also used TBAB as a solo catalyst, which shows a conversion of 29% (Table 1 Sl. no. 5), and when TBAB is mixed with the precursor MOF, Zr-DMBD, it shows a conversion of 66% (Table 1 Sl. no. 8). The catalytic potential of Ag(ɪ)-functionalized thiol MOFs (Zr-DMBD–Ag(ɪ)) was also investigated, but only at room temperature, where they were found to achieve a conversion of 32%; this catalysis was avoided at high temperatures, which would have led to their decomposition and the formation of nanoparticles in the reaction mixture (Table 1 Sl. no. 9), where the nanoparticle functionalized catalyst Ag@Zr-DMBD shows a comparatively high conversion of 38% at room temperature in 8 h (Table 1 Sl. no. 11). Finally, the reaction demonstrated maximal conversion of epichlorohydrin to the corresponding cyclic carbonate for 5 mmol of substrate when carried out using 10 mg of the Ag@Zr-DMBD cata-

Table 1 Screening of the catalyst for the cycloaddition of epichlorohydrin and CO_2

Sl. no.	Catalyst	Temperature (°C)	Time (h)	Conversion (%)
1	—	60	8	—
2	$ZrCl_4$	60	8	—
3	H_2DMBD	60	8	—
4	$AgNO_3$	60	8	20
5	TBAB	60	8	29
6	$AgNO_3$/TBAB	60	8	47
7	Zr-DMBD	60	8	36
8	Zr-DMBD/TBAB	60	8	66
9	Zr-DMBD–Ag(ɪ)/TBAB	RT	8	32
10	Ag@Zr-DMBD	60	8	51
11	Ag@Zr-DMBD/TBAB	RT	8	38
12	Ag@Zr-DMBD/TBAB	60	8	>99

Reaction conditions: 5 mmol epichlorohydrin, catalyst 10 mg, co-catalyst (TBAB) 2 mol%, atmospheric pressure (CO_2 balloon).

lyst combined with TBAB (2 mol%) at 60 °C and 1 bar CO_2 pressure for 8 hours (Table 1 Sl. no. 12 and Fig. S9†).

It is worth noting that a wide range of metal–organic frameworks (MOFs) and zeolitic imidazolate frameworks (ZIFs) containing Lewis acidic and nanoparticle (NP) sites are used for CO_2 fixation reactions, and many of these show catalytic activity in the presence of solvents and under high temperature and pressure conditions (as summarised in Table S1†). The thiol MOF based catalyst Ag@Zr-DMBD is utilized for CO_2 fixation reactions, and the results demonstrate comparable activity with that of reported benchmark catalysts.[82]

Optimization and kinetics study

Since temperature is a major component for thermodynamically and kinetically regulated products, the reaction was carried out at varying temperatures to optimize it, keeping the amount of the catalyst and co-catalyst constant. To stop the formation of unintended by-products (diols),[93] the reaction was carried out at relatively low temperatures *viz.*, 30, 40, 50, and 60 °C, resulting in 38, 73, 90, and 99% conversions of epichlorohydrin to cyclic carbonate, respectively, in 8 hours, which was examined by proton NMR of the reaction mixture (Fig. 4a). At 60 °C, a similar kinetics study with varying time intervals yielded 34% conversion after 2 hours, 60% conversion after 4 hours, 85% conversion after 6 hours, and 99% conversion after 8 hours, as confirmed by proton NMR (Fig. 4b).

After fixing the two significant parameters of the reaction, temperature and time, the kinetics of the reaction was also studied to optimize the amount of catalyst and the amount of co-catalyst (TBAB). The co-catalyst is a very important factor in

this reaction; on changing the mol% of TBAB, the reaction conversion changes, showing 60, 76, 90 and maximum conversion of 99% for 0.5, 1, 1.5 and 2 mol% of the co-catalyst (Fig. 4c) as observed by NMR spectroscopy (Fig. S9†). The catalyst shows maximum conversion with 10 mg catalyst when all other parameters are constant, and when 4, 6 and 8 mg of the catalyst was used for the reaction, it shows conversions of 49, 59, and 85%, respectively (Fig. 4d), as observed from NMR spectra (Fig. S10†).

Catalyst recyclability and substrate scope

Ideally, heterogeneous catalysts have to be chemically stable and reusable. In this case, the synthesized catalyst is stable in the reaction media and recyclable for up to four cycles, but after the fourth round of recycling, conversion slightly reduces to 96% (Fig. 5a). The catalyst shows 99, 99, 98 and 96% conversion from the 1st to 4th cycle, respectively (Fig. S18†). This experiment was performed thrice and it exhibited minimal standard deviation. The recyclability of the catalyst was tested by extracting the catalyst by centrifugation, washing it with methanol, and reusing it after drying at 60 °C for 12 h. The PXRD of the catalyst was tested after 1st and 4th cycles. After the 1st cycle, the crystallinity remains almost similar to that of the parent catalyst, and after the 4th cycle, the crystallinity decreases, although the characteristic PXRD peaks are almost identical (Fig. S19a†). The IR spectra of the catalyst were also collected after 1st and 4th cycles, and no significant changes were observed (Fig. S19b†). The catalyst leaching test was performed by the hot filtration method where the catalyst was filtered after 2 h and the reaction continued for another 8 h; only a negligible increase in catalytic conversion (due to TBAB) was observed, which ruled out the possibility of leaching (Fig. 5b). SEM-EDX analysis shows near identical Ag amount in the catalyst after the catalysis reaction, which supports the non-leaching behaviour of the catalyst (Fig. S20†).

To examine the versatility of the catalyst, a range of terminal epoxide substrates were examined under the optimized conditions. Since our model reaction was based on a liquid substrate, epichlorohydrin, different liquid substrates were chosen to cover a wide range of substrate scope (Table 2). High conversions such as 99% and 94% were observed for propylene oxide (Fig. S12†) and 1,2-epoxybutane (Fig. S13†), but the conversion decreases *i.e.* 90% for the substrate 1,2-epoxyhexane (Fig. S14†), 60% for styrene oxide (Fig. S15†) and 50% for 1,2-cyclohexane oxide (Fig. S16†). The decreasing trend of conversion can be explained by electronic and steric factors.[94] The ring-opening of epoxide is considered as the rate-determining step in the cycloaddition process. The electron-withdrawing properties of the chloromethyl group in epichlorohydrin make this process easier and result in high conversion values compared to those of the electron-donating group containing substrates. The steric hindrance increases from propylene oxide to 1,2-epoxyhexane with increasing chain length of the aliphatic moiety and leads to a decline in conversion. Similarly, the bulky phenyl group in styrene oxide and two rings in 1,2-cyclohexane oxide enhanced the steric crowding and decreased the
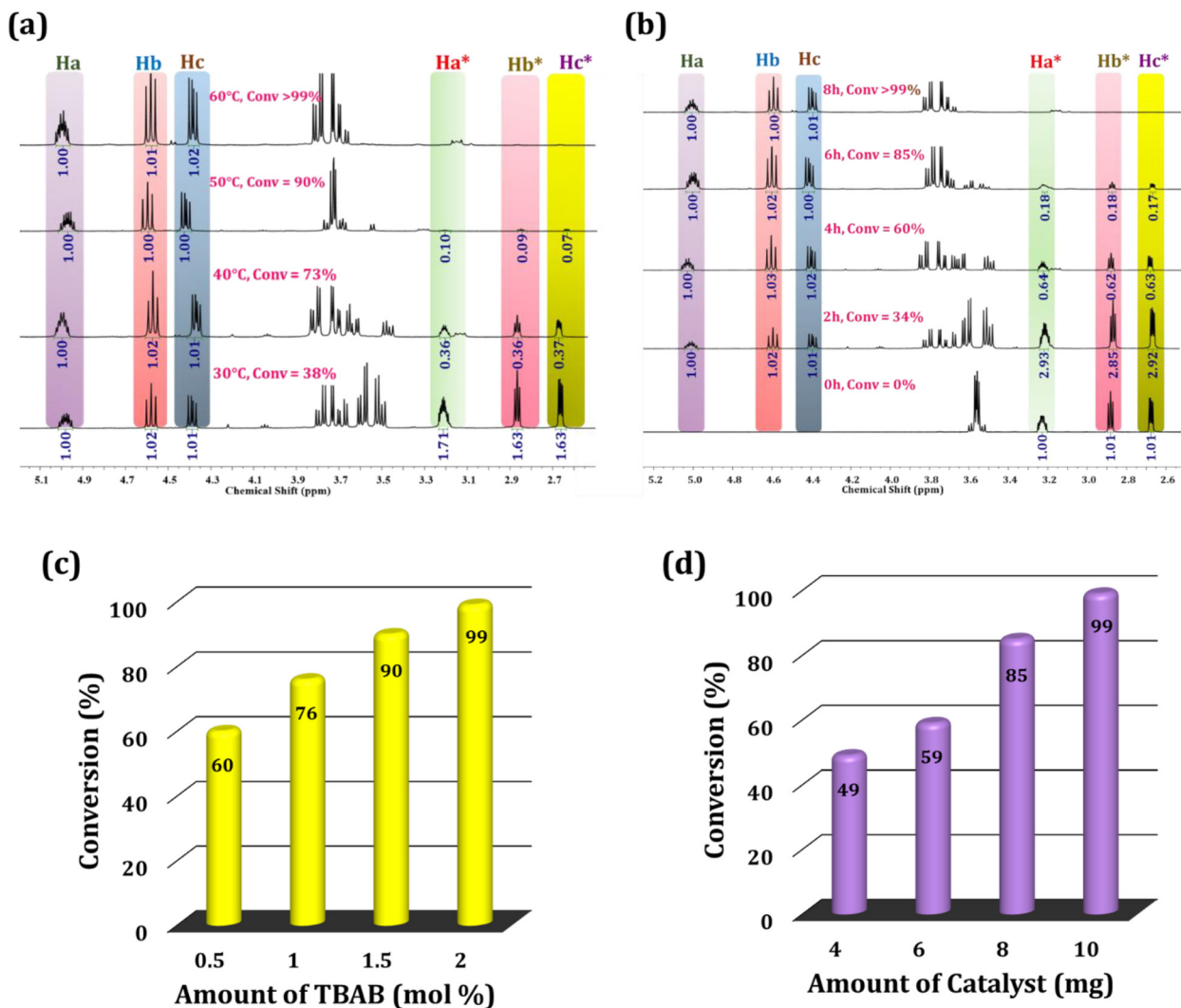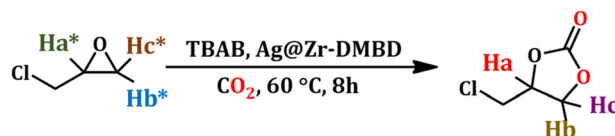
Fig. 4 ^{1}H NMR (CDCl$_3$, 400 MHz) spectra for the cycloaddition of epichlorohydrin with Ag@Zr–DMBD with respect to (a) temperature and (b) time (kinetic study). Conversion of epichlorohydrin with respect to (c) co-catalyst (TBAB) and (d) catalyst amounts represented by a bar diagram.

conversion. The synthesis of α-alkylidene cyclic carbonates from propargylic alcohol is another vital area of CO_2 fixation.[95,96] Silver-based catalysts have been utilized owing to their efficiency in converting propargylic alcohol to the corresponding cyclic carbonates.[97,98] The alkynophilic silver centre of the catalyst interacts with the C≡C of propargylic alcohols and polarizes the alkyne bond, which leads to cyclic carbonates in the presence of 1,8-diazabicyclo[5.4.0]undec-7-ene (DBU) and a CO_2 balloon.[18,99] To utilize the alkynophilic nature of Ag@Zr–DMBD, we examined our catalyst for the conversion of propargylic alcohol (2-methyl-3-butyn-2-ol) to the corresponding cyclic carbonate, which showed 60% conversion in 24 h at 60 °C and complete conversion in 48 h (Fig. S17†).

Proposed mechanism

Based on our result for the formation of cyclic carbonates from terminal epoxides and following the related literature, a mechanism is proposed (Fig. 6).[53,78,85,86] The catalytically active Zr,Ag centre of the thiol MOF catalyst acts as an active centre and synergistically binds with the electron-rich oxygen atom of the terminal epoxide.[53,78,85,86,88,100,101] Then the bromide ion of the co-catalyst TBAB reacts with the α-carbon of the polarised epoxy ring to open it, which then readily reacts with CO_2 to form an intermediate anion. This intermediate anion is prone to ring closing, which forms cyclic carbonate with the regeneration of the catalyst.
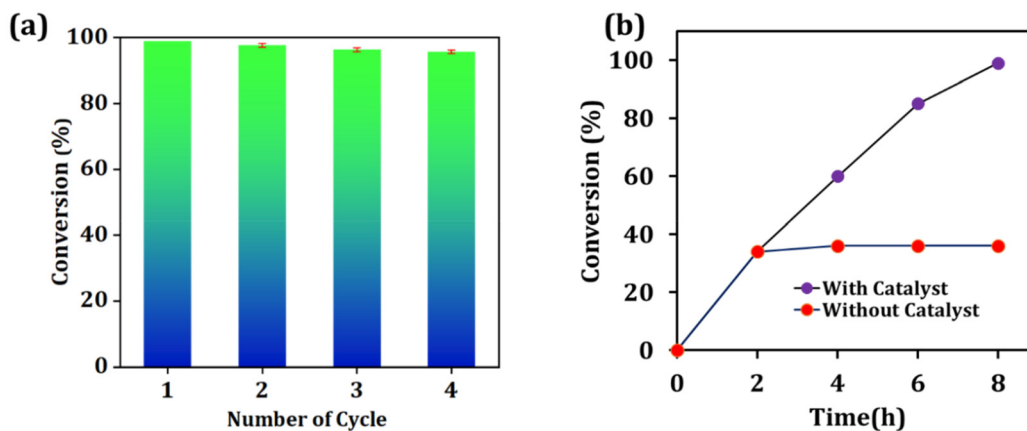
Fig. 5 (a) Recyclability test (error bars correspond to standard deviation) and (b) leaching test of the catalyst in the model reaction.

Table 2 Substrate scope for the catalytic system Ag@Zr–DMBD/TBAB

Sl. no.	Substrate	Product	Temp (°C)	Time (h)	Conversion (%)
1			60	8	99
2			60	8	94
3			60	8	90
4			60	8	60
5			60	8	50

Reaction conditions: terminal epoxide (5 mmol), TBAB (2 mol%), Ag@Zr–DMBD (10 mg), 60 °C, CO_2 atmospheric pressure (1 bar).
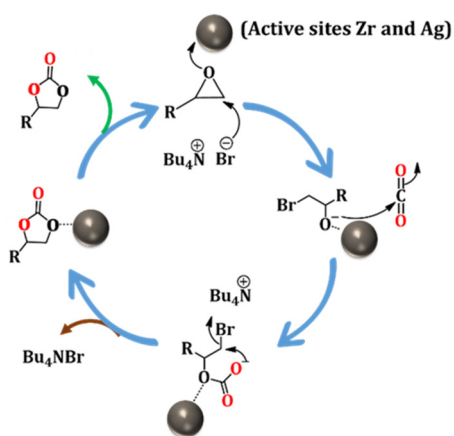

Fig. 6 Proposed reaction mechanism of the cycloaddition reaction between CO_2 and terminal epoxide by the catalyst Ag@Zr–DMBD and co-catalyst.

Conclusion

In conclusion, we have accomplished the synthesis of the silver nanoparticle functionalized thiol MOF-based heterogeneous catalyst Ag@Zr-DMBD by utilizing the free-standing thiol group of the well-known stable thiol MOF Zr-DMBD and used it for CO_2 fixation reactions. The catalyst can convert the terminal epoxide epichlorohydrin to the corresponding cyclic carbonate in 8 h and can convert a wide range of terminal epoxide substrates with good conversion capacity. This study shows the utilization of a thiol MOF as a heterogeneous catalyst by functionalizing it with a catalytically active metal centre. In comparison to other functional group containing MOFs, thiol MOFs are less explored because of the scarcity of thiol-based ligands and their tedious synthetic procedure, but the presence of the free sanding thiol group in the thiol MOF framework makes it attractive for post-synthetic modifications.

Previous reports on thiol-based MOFs rarely explored the heterogeneous catalytic activity of thiol MOF-based compounds. In brief, this work shows a feasible method for using a thiol MOF for Ag nanoparticle functionalization and utilization in CO_2 fixation reactions, which further boosts efficiency compared to that of the parent thiol MOF Zr-DMBD.

Author contributions

R. P.: Conceptualization, investigation, methodology, and writing – original draft; D. S.: Conceptualization, supervision, writing, editing, and funding acquisition.

Conflicts of interest

There are no conflicts of interest.

Acknowledgements

References

1 H. Furukawa, K. E. Cordova, M. O'Keeffe and O. M. Yaghi, *Science*, 2013, **341**, 1230444.

2 H. Li, M. Eddaoudi, M. O'Keeffe and O. M. Yaghi, *Nature*, 1999, **402**, 276–279.

3 J. L. Rowsell and O. M. Yaghi, *Microporous Mesoporous Mater.*, 2004, **73**, 3–14.

4 S. Kitagawa, *Chem. Soc. Rev.*, 2014, **43**, 5415–5418.

5 N. Stock and S. Biswas, *Chem. Rev.*, 2012, **112**, 933–969.

6 M. D. Allendorf, V. Stavila, M. Witman, C. K. Brozek and C. H. Hendon, *J. Am. Chem. Soc.*, 2021, **143**, 6705–6723.

7 X. Zhang, Z. Chen, X. Liu, S. L. Hanna, X. Wang, R. Taheri-Ledari, A. Maleki, P. Li and O. K. Farha, *Chem. Soc. Rev.*, 2020, **49**, 7406–7427.

8 O. K. Farha, I. Eryazici, N. C. Jeong, B. G. Hauser, C. E. Wilmer, A. A. Sarjeant, R. Q. Snurr, S. T. Nguyen, A. O. Z. R. Yazaydın and J. T. Hupp, *J. Am. Chem. Soc.*, 2012, **134**, 15016–15021.

9 D. Wu, P.-F. Zhang, G.-P. Yang, L. Hou, W.-Y. Zhang, Y.-F. Han, P. Liu and Y.-Y. Wang, *Coord. Chem. Rev.*, 2021, **434**, 213709.

10 Y. He, W. Zhou, G. Qian and B. Chen, *Chem. Soc. Rev.*, 2014, **43**, 5657–5678.

11 R. Sahoo and M. C. Das, *Coord. Chem. Rev.*, 2021, **442**, 213998.

12 D.-W. Lim and H. Kitagawa, *Chem. Soc. Rev.*, 2021, **50**, 6349–6368.

13 H. D. Lawson, S. P. Walton and C. Chan, *ACS Appl. Mater. Interfaces*, 2021, **13**, 7004–7020.

14 J. Lee, O. K. Farha, J. Roberts, K. A. Scheidt, S. T. Nguyen and J. T. Hupp, *Chem. Soc. Rev.*, 2009, **38**, 1450–1459.

15 V. Pascanu, G. González Miera, A. K. Inge and B. Martín-Matute, *J. Am. Chem. Soc.*, 2019, **141**, 7223–7234.

16 Y.-S. Wei, M. Zhang, R. Zou and Q. Xu, *Chem. Rev.*, 2020, **120**, 12089–12174.

17 J. Guo, Y. Qin, Y. Zhu, X. Zhang, C. Long, M. Zhao and Z. Tang, *Chem. Soc. Rev.*, 2021, **50**, 5366–5396.

18 R. Das, V. Parihar and C. Nagaraja, *Inorg. Chem. Front.*, 2022, **9**, 2583–2593.

19 L. E. Kreno, K. Leong, O. K. Farha, M. Allendorf, R. P. Van Duyne and J. T. Hupp, *Chem. Rev.*, 2012, **112**, 1105–1125.

20 S. Bhattacharyya, A. Chakraborty, K. Jayaramulu, A. Hazra and T. K. Maji, *Chem. Commun.*, 2014, **50**, 13567–13570.

21 P. Mahata, S. K. Mondal, D. K. Singha and P. Majee, *Dalton Trans.*, 2017, **46**, 301–328.

22 S. Khatua, S. Goswami, S. Biswas, K. Tomar, H. S. Jena and S. Konar, *Chem. Mater.*, 2015, **27**, 5349–5360.

23 S. Sahoo, S. Mondal and D. Sarma, *Coord. Chem. Rev.*, 2022, **470**, 214707.

24 H.-Y. Li, S.-N. Zhao, S.-Q. Zang and J. Li, *Chem. Soc. Rev.*, 2020, **49**, 6364–6401.

25 S. Mandal, S. Natarajan, P. Mani and A. Pankajakshan, *Adv. Funct. Mater.*, 2021, **31**, 2006291.

26 A. V. Desai, B. Manna, A. Karmakar, A. Sahu and S. K. Ghosh, *Angew. Chem.*, 2016, **128**, 7942–7946.

27 D. Sarma, M. Prabu, S. Biju, M. L. P. Reddy and S. Natarajan, *Eur. J. Inorg. Chem.*, 2010, 3813–3822.

28 A. Schneemann, Y. Jing, J. D. Evans, T. Toyao, Y. Hijikata, Y. Kamiya, K.-I. Shimizu, N. C. Burtch and S.-I. Noro, *Dalton Trans.*, 2021, **50**, 10423–10435.

29 M. Joharian, A. Morsali, A. A. Tehrani, L. Carlucci and D. M. Proserpio, *Green Chem.*, 2018, **20**, 5336–5345.

30 Z. Sharifzadeh and A. Morsali, *Coord. Chem. Rev.*, 2022, **459**, 214445.

31 P. V. Dau, K. K. Tanabe and S. M. Cohen, *Chem. Commun.*, 2012, **48**, 9370–9372.

32 K.-K. Yee, N. Reimer, J. Liu, S.-Y. Cheng, S.-M. Yiu, J. Weber, N. Stock and Z. Xu, *J. Am. Chem. Soc.*, 2013, **135**, 7795–7798.

33 S. Chowdhury, P. Sharma, K. Kundu, P. P. Das, P. Rathi and P. F. Siril, *Inorg. Chem.*, 2023, **62**, 3875–3885.

34 K. Ulrich and U. Jakob, *Free Radical Biol. Med.*, 2019, **140**, 14–27.

35 G. Bulaj, T. Kortemme and D. P. Goldenberg, *Biochemistry*, 1998, **37**, 8965–8972.

36 N. M. Giles, A. B. Watts, G. I. Giles, F. H. Fry, J. A. Littlechild and C. Jacob, *Chem. Biol.*, 2003, **10**, 677–693.

37 K. I. Willig, S. O. Rizzoli, V. Westphal, R. Jahn and S. W. Hell, *Nature*, 2006, **440**, 935–939.

38 H. S. Jiang, Y. Zhang, Z. W. Lu, R. Lebrun, B. Gontero and W. Li, *Small*, 2019, **15**, 1900860.

39 X. Deng, S.-L. Zheng, Y.-H. Zhong, J. Hu, L.-H. Chung and J. He, *Coord. Chem. Rev.*, 2022, **450**, 214235.

40 Y.-L. Wong, Y. Diao, J. He, M. Zeller and Z. Xu, *Inorg. Chem.*, 2018, **58**, 1462–1468.

41 M.-Q. Li, Y.-L. Wong, T.-S. Lum, K. S.-Y. Leung, P. K. Lam and Z. Xu, *J. Mater. Chem. A*, 2018, **6**, 14566–14570.

42 J. H. Cavka, S. Jakobsen, U. Olsbye, N. Guillou, C. Lamberti, S. Bordiga and K. P. Lillerud, *J. Am. Chem. Soc.*, 2008, **130**, 13850–13851.

43 D. C. Liu, T. Ouyang, R. Xiao, W. J. Liu, D. C. Zhong, Z. Xu and T. B. Lu, *ChemSusChem*, 2019, **12**, 2166–2170.

44 K.-K. Yee, Y.-L. Wong, M. Zha, R. Y. Adhikari, M. T. Tuominen, J. He and Z. Xu, *Chem. Commun.*, 2015, **51**, 10941–10944.

45 Y. Wang, X. Zhu, X. Zhang, J. Zheng, H. Li, N. Xie, Y. Guo, H.-B. Sun and G. Zhang, *Dalton Trans.*, 2022, **51**, 4043–4051.

46 L. Ding, X. Luo, P. Shao, J. Yang and D. Sun, *ACS Sustainable Chem. Eng.*, 2018, **6**, 8494–8502.

47 W. J. Phang, H. Jo, W. R. Lee, J. H. Song, K. Yoo, B. Kim and C. S. Hong, *Angew. Chem.*, 2015, **127**, 5231–5235.

48 K.-K. Yee, Y.-L. Wong and Z. Xu, *Dalton Trans.*, 2016, **45**, 5334–5338.

49 R. Khatun, P. Bhanja, P. Mondal, A. Bhaumik, D. Das and S. M. Islam, *New J. Chem.*, 2017, **41**, 12937–12946.

50 L.-X. You, S.-X. Yao, B.-B. Zhao, G. Xiong, I. Dragutan, V. Dragutan, X.-G. Liu, F. Ding and Y.-G. Sun, *Dalton Trans.*, 2020, **49**, 6368–6376.

51 Z. Zhang, H. Gao, H. Wu, Y. Qian, L. Chen and J. Chen, *ACS Appl. Nano Mater.*, 2018, **1**, 6463–6476.

52 F. Pourhassan, R. Khalifeh and H. Eshghi, *Fuel*, 2021, **287**, 119567.

53 Y.-L. Wu, G.-P. Yang, S. Cheng, J. Qian, D. Fan and Y.-Y. Wang, *ACS Appl. Mater. Interfaces*, 2019, **11**, 47437–47445.

54 W. F. Ruddiman, *Sci. Am.*, 2005, **292**, 46–53.

55 D. C. Harris, *Anal. Chem.*, 2010, **82**, 7865–7870.

56 R. A. Maia, B. Louis, W. Gao and Q. Wang, *React. Chem. Eng.*, 2021, **6**, 1118–1133.

57 M. Z. Jacobson, *Energy Environ. Sci.*, 2009, **2**, 148–173.

58 M. Sai Bhargava Reddy, D. Ponnamma, K. K. Sadasivuni, B. Kumar and A. M. Abdullah, *RSC Adv.*, 2021, **11**, 12658–12681.

59 B. Yao, T. Xiao, O. A. Makgae, X. Jie, S. Gonzalez-Cortes, S. Guan, A. I. Kirkland, J. R. Dilworth, H. A. Al-Megren, S. M. Alshihri, P. J. Dobson, G. P. Owen, J. M. Thomas and P. P. Edwards, *Nat. Commun.*, 2020, **11**, 6395.

60 M. Aresta, A. Dibenedetto and A. Angelini, *Chem. Rev.*, 2014, **114**, 1709–1742.

61 N. Alam, N. Ojha, S. Kumar and D. Sarma, *ACS Sustainable Chem. Eng.*, 2023, **11**, 2658–2669.

62 A. M. Appel, J. E. Bercaw, A. B. Bocarsly, H. Dobbek, D. L. DuBois, M. Dupuis, J. G. Ferry, E. Fujita, R. Hille, P. J. A. Kenis, C. A. Kerfeld, R. H. Morris, C. H. F. Peden, A. R. Portis, S. W. Ragsdale, T. B. Rauchfuss, J. N. H. Reek, L. C. Seefeldt, R. K. Thauer and G. L. Waldrop, *Chem. Rev.*, 2013, **113**, 6621–6658.

63 M. Mikkelsen, M. Jørgensen and F. C. Krebs, *Energy Environ. Sci.*, 2010, **3**, 43–81.

64 D. M. D'Alessandro, B. Smit and J. R. Long, *Angew. Chem., Int. Ed.*, 2010, **49**, 6058–6082.

65 F. N. Al-Rowaili, U. Zahid, S. Onaizi, M. Khaled, A. Jamal and E. M. Al-Mutairi, *J. CO_2 Util.*, 2021, **53**, 101715.

66 Y. Zhao, B. Yu, Z. Yang, H. Zhang, L. Hao, X. Gao and Z. Liu, *Angew. Chem., Int. Ed.*, 2014, **53**, 5922–5925.

67 T. K. Pal, D. De and P. K. Bharadwaj, *Coord. Chem. Rev.*, 2020, **408**, 213173.

68 D. Liu, G. Li, J. Liu, Y. Wei and H. Guo, *ACS Appl. Mater. Interfaces*, 2018, **10**, 22119–22129.

69 M. H. Alkordi, Ł. J. Weseliński, V. D'Elia, S. Barman, A. Cadiau, M. N. Hedhili, A. J. Cairns, R. G. AbdulHalim, J.-M. Basset and M. Eddaoudi, *J. Mater. Chem. A*, 2016, **4**, 7453–7460.

70 M. Yin, L. Wang and S. Tang, *ACS Appl. Mater. Interfaces*, 2022, **14**, 55674–55685.

71 G. Singh and C. M. Nagaraja, *J. CO_2 Util.*, 2021, **53**, 101716.

72 R. Das, T. Ezhil and C. M. Nagaraja, *Cryst. Growth Des.*, 2022, **22**, 598–607.

73 P. T. K. Nguyen, H. T. D. Nguyen, H. N. Nguyen, C. A. Trickett, Q. T. Ton, E. Gutiérrez-Puebla, M. A. Monge, K. E. Cordova and F. Gándara, *ACS Appl. Mater. Interfaces*, 2018, **10**, 733–744.

74 L. Wang, W. Qiao, H. Liu, S. Li, J. Wu and H. Hou, *Inorg. Chem.*, 2023, **62**, 3817–3826.

75 S. Sahoo and D. Sarma, *Cryst. Growth Des.*, 2022, **22**, 5645–5657.

76 Z. Xu, Y.-Y. Zhao, L. Chen, C.-Y. Zhu, P. Li, W. Gao, J.-Y. Li and X.-M. Zhang, *Dalton Trans.*, 2023, **52**, 3671–3681.

77 S. Sahoo, S. Mondal and D. Sarma, *Eur. J. Inorg. Chem.*, 2023, **26**, e202300067.

78 M. Singh, P. Solanki, P. Patel, A. Mondal and S. Neogi, *Inorg. Chem.*, 2019, **58**, 8100–8110.

79 S. Verma, R. B. N. Baig, M. N. Nadagouda and R. S. Varma, *Green Chem.*, 2016, **18**, 4855–4858.

80 R. Das and C. M. Nagaraja, *Inorg. Chem.*, 2020, **59**, 9765–9773.

81 S. Chatterjee, S. Das, P. Bhanja, E. S. Erakulan, R. Thapa, S. Ruidas, S. Chongdar, S. Ray and A. Bhaumik, *J. CO2 Util.*, 2022, **55**, 101843.

82 N.-N. Zhu, X.-H. Liu, T. Li, J.-G. Ma, P. Cheng and G.-M. Yang, *Inorg. Chem.*, 2017, **56**, 3414–3420.

83 X. Liu, C. Hu, J. Wu, H. Zhu, Y. Li, P. Cui and F. Wei, *J. Solid State Chem.*, 2021, **296**, 121889.

84 D. Wu, X. Lu, Y. Tang, F. Gao, G. Yang and Y.-Y. Wang, *ACS Appl. Nano Mater.*, 2023, **6**, 6197–6207.

85 C.-Y. Gao, C. Mao, Y. Yang, N. Xu, J. Liu, X. Chen, J. Liu and L. Duan, *CrystEngComm*, 2023, **25**, 108–113.

86 K. S. Keshri, S. Bhattacharjee, A. Singha, A. Bhaumik and B. Chowdhury, *Mol. Catal.*, 2022, **522**, 112234.

87 Z. Taşcı, A. Kunduracıoğlu, İ. Kani and B. Çetinkaya, *ChemCatChem*, 2012, **4**, 831–835.

88 J. Jin, J. Xue, D. Wu, G. Yang and Y. Wang, *Chem. Commun.*, 2022, **58**, 7749–7752.

89 G. Li, X. Sui, X. Cai, W. Hu, X. Liu, M. Chen and Y. Zhu, *Angew. Chem., Int. Ed.*, 2021, **60**, 10573–10576.

90 L. Vial, R. F. Ludlow, J. Leclaire, R. Pérez-Fernández and S. Otto, *J. Am. Chem. Soc.*, 2006, **128**, 10253–10257.

91 R. K. Aparna, S. Mukherjee, S. S. Rose and S. Mandal, *Inorg. Chem.*, 2022, **61**, 16441–16447.

92 D. Sarma, C. D. Malliakas, K. S. Subrahmanyam, S. M. Islam and M. G. Kanatzidis, *Chem. Sci.*, 2016, **7**, 1121–1132.

93 E. E. Macias, P. Ratnasamy and M. A. Carreon, *Catal. Today*, 2012, **198**, 215–218.

94 X. Gao, M. Liu, J. Lan, L. Liang, X. Zhang and J. Sun, *Cryst. Growth Des.*, 2017, **17**, 51–57.

95 X. Yu, Z. Yang, F. Zhang, Z. Liu, P. Yang, H. Zhang, B. Yu, Y. Zhao and Z. Liu, *Chem. Commun.*, 2019, **55**, 12475–12478.

96 R. Das and C. M. Nagaraja, *Green Chem.*, 2021, **23**, 5195–5204.

97 D. Chakraborty, P. Shekhar, H. D. Singh, R. Kushwaha, C. P. Vinod and R. Vaidhyanathan, *Chem. – Asian J.*, 2019, **14**, 4767–4773.

98 S. Ghosh, R. A. Molla, U. Kayal, A. Bhaumik and S. M. Islam, *Dalton Trans.*, 2019, **48**, 4657–4666.

99 H. Yang, X. Zhang, G. Zhang and H. Fei, *Chem. Commun.*, 2018, **54**, 4469–4472.

100 X. Liu, C. Hu, J. Wu, H. Zhu, Y. Li, P. Cui and F. Wei, *J. Solid State Chem.*, 2021, **296**, 121889.

101 Z. Gao, L. Liang, X. Zhang, P. Xu and J. Sun, *ACS Appl. Mater. Interfaces*, 2021, **13**, 61334–61345.